Zintl Phases

DOI: 10.1002/ange.201301540

$LiBSi_2$: A Tetrahedral Semiconductor Framework from Boron and Silicon Atoms Bearing Lithium Atoms in the Channels**

Michael Zeilinger, Leo van Wüllen, Daryn Benson, Verina F. Kranak, Sumit Konar, Thomas F. Fässler, and Ulrich Häussermann**

Dedicated to Prof. Dr. Dr. h. c. mult. Wolfgang A. Herrmann on the occasion of his 65th birthday

The crystalline open frameworks of zeolites and clathrates are based on three-periodic, four-connected nets with tetrahedral nodes and have long attracted attention for their unique physical properties and great significance to fundamental crystal chemistry.[1] Such open tetrahedral frameworks (OTFs) enclose interstitial volumes in the form of large and separated cages (clathratic frameworks) or channels (zeolitic frameworks). While they most commonly occur with oxide materials, using oxygen to bridge the tetrahedral nodes, intermetallic Zintl phases may realize OTFs where the edges of nets correspond to covalent two-center, two-electron bonds (direct links).[2] Tetrahedral nodes in Zintl-phase OTFs are typically represented by the tetravalent Group 14 element (Tt) atoms Si, Ge, and Sn or mixtures of Tt atoms and trivalent Group 13 element (Tr) atoms (sp^3 hybridized atoms). For the latter systems, the apparent electron deficiency is balanced by electrons of the less electronegative metals situated in cavities in the OTF (guest species), which becomes nominally charged, that is, $(4c\text{-}Tt)_n = (A^+)_m(4c\text{-}Tt)_{n-m}(4c\text{-}Tr^-)_m$ (4c = four-connected, A = alkaline-earth metal) and thus shows a strong analogy to the charge distribution in aluminosilicates.

Among Zintl-phase OTFs the clathrate-I and -II type of structures with the nets **mtn** and **mep**, respectively,[3] are most prominent (Scheme 1). They occur for numerous compositions and have received considerable attention for their thermoelectric and superconducting properties.[4] Guest species in cages (i.e. Na–Cs, Sr, Ba, Eu atoms) play an important role in determining and tuning electric and thermal transport properties.[2a] Other OTFs include zeolitic frameworks such as the chiral net **unj** which is the basis of the structures of $NaInSn_2$, $NaGaSn_2$, and $NaGaSn_5$ as well as *hP*-Na_2ZnSn_5 and *tI*-Na_2ZnSn_5,[5] and **CAS** which describes the topology of the frameworks of $Eu_4Ga_6Si_{16}$ or ASi_6 (A = Ca, Sr, Ba).[6]

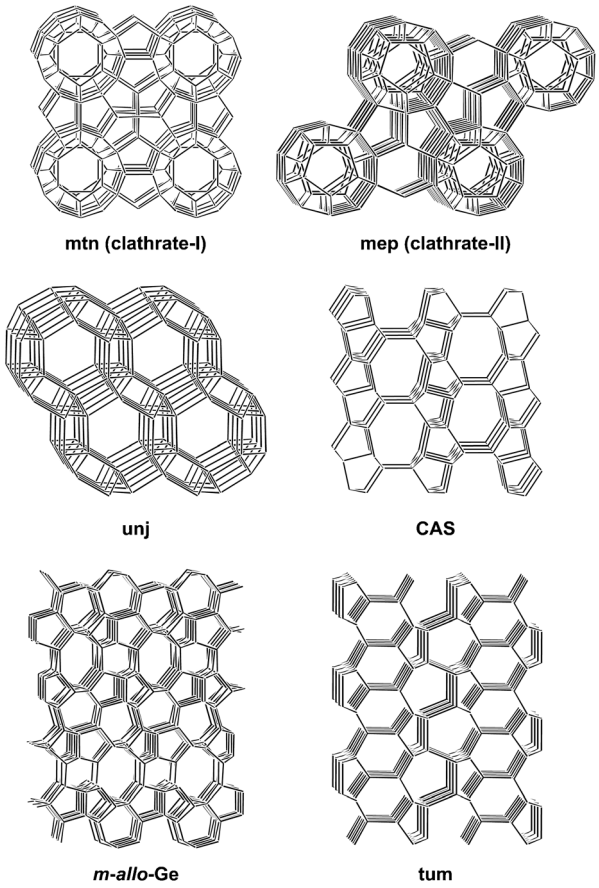

Scheme 1. Open tetrahedral frameworks realized by Zintl phases and Group 14 elements.[3]

Notably, compared with silicates the topological variety of Zintl-phase OTFs is very limited[3a,7] and especially attempts to achieve Zintl-phase OTFs with Li as the guest species have long been unsuccessful,[8] although interesting properties for such materials were predicted.[9] For clathratic frameworks it

[*] M. Zeilinger, Prof. Dr. T. F. Fässler
Department of Chemistry, Technische Universität München, Lichtenbergstrasse 4, 85747 Garching/München (Germany)
E-mail: thomas.faessler@lrz.tum.de
Prof. Dr. L. van Wüllen
Department of Physics, University of Augsburg, Universitätsstrasse 1, 86159 Augsburg (Germany)
D. Benson
Department of Physics, Arizona State University, Tempe, Arizona 85287-1504 (USA)
V. F. Kranak, S. Konar, Prof. Dr. U. Häussermann
Department of Materials and Environmental Chemistry, Stockholm University, SE-10691 Stockholm (Sweden)
E-mail: Ulrich.Haussermann@mmk.su.se

[**] This work was supported by Fonds der Chemischen Industrie, TUM Graduate School, Deutsche Forschungsgemeinschaft FA 198/11-1, the Swedish Research Council under contract number 2010-4827, and the National Science Foundation through grant DMR-1007557.

Supporting information for this article (including further details on the synthesis procedure, the analysis of products, and the computational procedure) is available on the WWW under http://dx.doi.org/10.1002/anie.201301540.

is believed that cages would be too large for Li atoms.[8] The encapsulation of Li atoms (in a stable compound) will probably require the OTF to consist of a large fraction of light elements from the second row, that is, B and C atoms. Thus far, the only known OTF involving a second row element is found in $K_7B_7Si_{39}$,[10] where a comparatively small fraction of the Si atoms in a clathrate-I structure are replaced by B atoms. Although this produced the smallest lattice parameter among Zintl phases with the clathrate-I structure cage, the size remained far too large for Li atoms.

Herein, we report on $LiBSi_2$ displaying a zeolitic framework with a new topology based on a unique strictly ordered distribution of B and Si atoms. This B-Si OTF has mutually orthogonal channels that host Li atoms.

$LiBSi_2$ was obtained as a dark gray, microcrystalline, powder from reaction mixtures LiB:Si = 1:1 that had been pressurized to 10 GPa and heated at 900 °C. $LiBSi_2$ is air and moisture stable, and also inert to strong acids. Its thermal stability exceeds 800 °C. The structure of $LiBSi_2$ depicted in Figure 1 was solved from powder X-ray diffraction data using a parallel tempering algorithm and subsequently finalized by Rietveld refinement.[11]

$LiBSi_2$ crystallizes with the tetragonal space group $P4_2/nmc$ and contains eight formula units in the unit cell

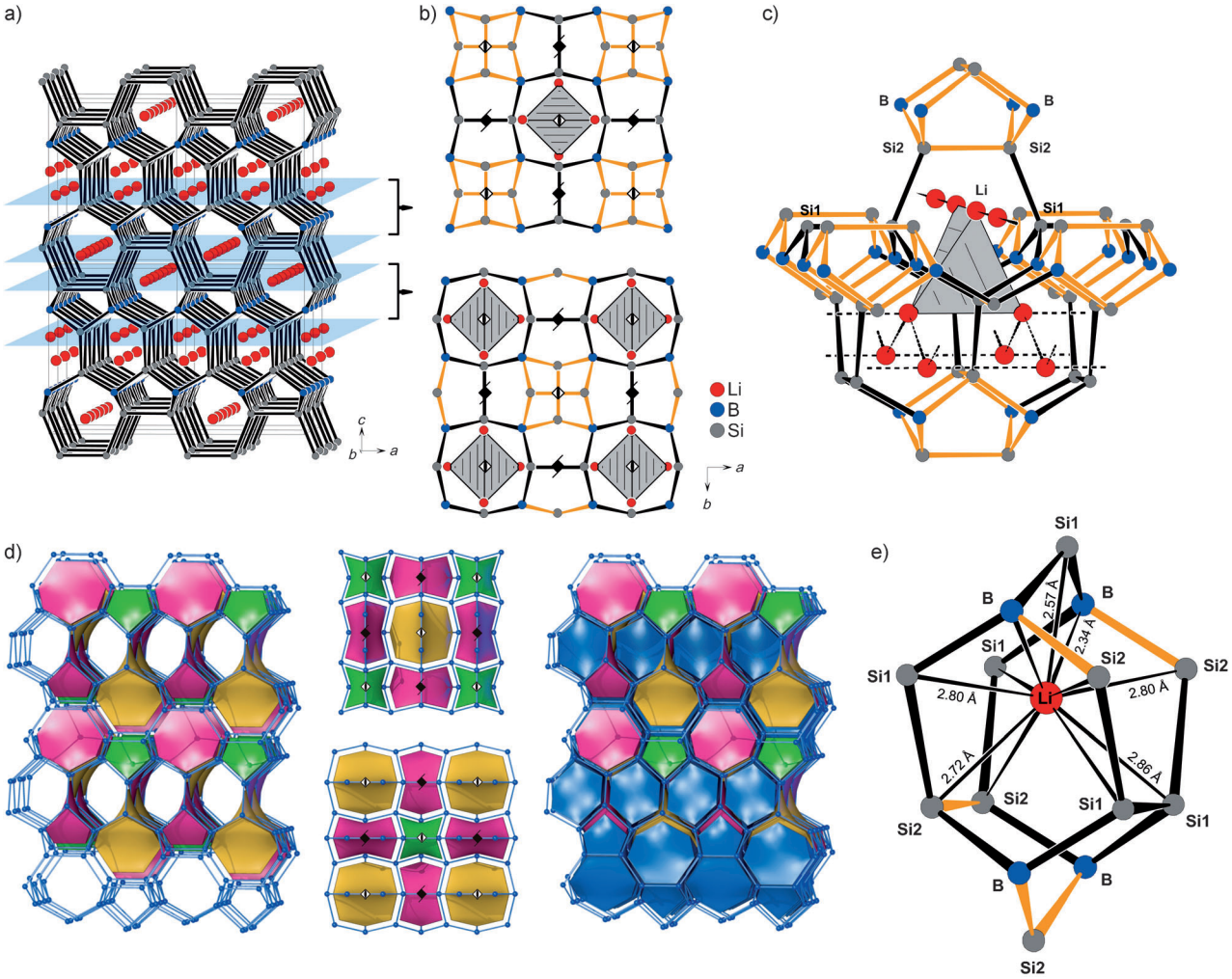

Figure 1. a) Crystal structure of tetragonal $LiBSi_2$ (2×2×2 supercell) viewed approximately along the [100] direction. Atoms are displayed as ellipsoids at a 90% probability (Li red, B blue, Si dark gray). Boundaries of two slab-like building units are marked by light blue planes. b) Two consecutive slab building units projected along the [001] direction. Bonds of the realgar-like $[B_4Si2_4]$ structural unit are drawn in yellow. Elongated tetrahedra produced by the arrangement of Li atoms are highlighted. The position of 4_2 and $\bar{4}$ axes are indicated by their symbol. c) Section of the $LiBSi_2$ structure showing the consequence of connecting slab building units: six- and seven-membered rings are introduced defining orthogonal channels that host the Li atoms. Within seven-ring channels Li atoms are arranged as linear chains, within six-ring channels as zigzag chains. Connecting lines between Li atoms do not indicate interactions, they are only meant to emphasize structural features. d) Natural tiling for the net **tum** formed by B and Si atoms in $LiBSi_2$. There are four different kinds of tiles, three four-faced tiles and one six-faced. (A tile is characterized by a face symbol $[M^m.N^n...]$ indicating that there are m faces that are M-rings, n faces that are N-rings, and so on). Left: Arrangement of 4-faced tiles $[5^4]$ (green), $[7^4]$ (yellow), and $[5^2.7^2]$ (pink) not sharing faces. Middle: Arrangement of four-faced tiles within slab building blocks (Figure 1b). Right: Complete natural tiling of **tum** including also the six-faced "Li tiles" $[5^2.6^2.7^2]$ (blue). Li tiles share common six-ring faces which emphasizes the six-ring channel system (hosting Li zigzag chains) in zeolitic $LiBSi_2$ (seen at the bottom of the figure). e) Coordination environment around Li atoms within a $[5^2.6^2.7^2]$ tile.

(Figure 1 a). The B-Si ordered OTF is built from three distinct crystallographic positions—one B site (8*f*) and two Si sites (Si1 and Si2, both on 8*g*)—and thus corresponds to a trinodal net. Li atoms are situated on an *8g* site and occupy channels in the B-Si OTF.

The tetrahedral B-Si framework can be divided into $[B_4Si2_4]$ realgar-like units and Si1-Si1 dumbbells which occur in a 1:2 ratio and are arranged in two-dimensional slabs (Figure 1 b). The realgar-like unit represents a cage, which is enclosed by four five-membered rings. Its linkage with the $Si1_2$ dumbbell units creates additional five-membered rings. The slab also contains eight-membered rings, which, however, become part of seven-membered rings upon connecting slabs and thus do not represent strong rings in the three-periodic framework.[12] Finally, a slab hosts mutually perpendicular linear chains of Li atoms at two different heights (corresponding to the thickness of a slab; Figure 1 a) running along the *a* and *b* directions. Distances in a linear chain are alternating short (3.36 Å) and long (3.47 Å), and the arrangement of short distances corresponds to elongated Li_4 tetrahedra surrounded by eight-membered rings.

In the three-periodic net, slabs are stacked along the *c* direction, related by the *n* glide perpendicular to *c* (Figure 1 b). As a consequence, realgar and Li_4 tetrahedral units are situated alternating on top of each other and $(Si1)_2$ dumbbells are stacked mutually rotated by 90°.[13] The connection of slabs introduces six- and seven-membered rings, which define the channels hosting the Li atoms (Figure 1 c, compared to Figure 1 a). In channels embraced by seven-membered rings, Li atoms are arranged as the linear chains mentioned above; in channels embraced by six-membered rings, Li atoms form zigzag chains where they are equidistantly separated at 3.66 Å (Figure 1 c). This distance corresponds to the separation of Li_4 tetrahedra, or alternatively the distance between parallel linear chains at different heights. Both kinds of channels run along the *a* and *b* directions and are mutually converted by a 90° rotation around the *c* axis.

The outcome of the ordering of B and Si atoms is that B atoms are exclusively bonded to Si atoms with $d_{Si\text{-}B} = 2.05$ and 2.08 Å whereas Si atoms utilize two homoatomic bonds with distances $d_{Si\text{-}Si} = 2.44$, 2.47, and 2.51 Å. Different B–Si and Si–Si bond lengths induce distorted tetrahedral coordination environments ($\sphericalangle$(Si–B–Si) = 91.07°–124.52°; $\sphericalangle$(B–Si–B) = 106.41°, 117.30°; $\sphericalangle$(Si–Si–B) = 100.94°–116.96°; $\sphericalangle$(Si–Si–Si) = 112.33°).

The OTF formed by B and Si atoms in $LiBSi_2$ consists exclusively of five-, six-, and seven-membered rings and represents a not yet described topology for a three-periodic, four-connected net. It has been assigned the symbol **tum** in the TTD topological database.[14] We note that **tum** is also the net of the orthorhombic framework of the recently discovered intermetallic compounds $Na_5M_{2+x}Sn_{10-x}$ ($x \approx 0.5$, M = Zn, Hg) where it is formed by the M and Sn atoms.[15]

The natural tiling associated with **tum** is shown in Figure 1 d. A tiling is the filling of space by generalized polyhedra (tiles) that share faces.[16] A tile represents the interior of a cage with typically curved faces that are rings of the net. Thus a tiling carries a net formed by the vertices and edges of tiles. According to a set of rules, natural tilings are unique and provide an unambiguous way to partition space by the net. This in turn enables convenient identification and analysis of the size and location of cavities and channels. For **tum** there are four kinds of tiles: one corresponds to the $[B_4Si2_4]$ realgar-like cage centered at the Wyckoff site 2a and has the face symbol $[5^4]$, indicating that there are four faces that are five-membered rings. Another tile with face symbol $[7^4]$ is located at the center of the Li_4 tetrahedron (position 2b) and a third tile with the face symbol $[5^2.7^2]$ is centered at site 4d, in between two $Si1_2$ dumbbells stacked along the *c* direction. The fourth tile is enclosed by six faces (face symbol $[5^2.6^2.7^2]$) and is centered at a position approximately corresponding to the location of the Li atoms (Figure 1 e).

This partitioning appears chemically meaningful; the three four-faced tiles do not share common faces but are tetrahedrally surrounded by Li tiles, which in turn are octahedrally connected to two $[5^2.7^2]$ tiles (through a seven- and a five-membered ring face, respectively), one realgar $[5^4]$ tile, one $[7^4]$ tile, and two other Li tiles (sharing six-sided faces). The face sharing of Li tiles defines the relevant channels (Figure 1 f), which, interestingly, are those that are embraced by six-membered rings and host zigzag chains of Li atoms rather than the ones embraced by seven-membered rings that host linear chains. Li atoms in $LiBSi_2$ attain a clearly defined coordination by two B and nine Si atoms (Figure 1 e). Distances range from 2.34 Å (Li-B) to 2.86 Å (Li-Si1) and are well separated from the next nearest neighbor distances starting off at 3.34 Å (Li-B). However, the tile (cage) associated with Li is larger (14 vertices) and Li is positioned quite off-centered in its tile.

The structure was further confirmed by the Raman spectrum of $LiBSi_2$ (Figure 2). The rather complex structure gives rise to 31 Raman-active modes,[17] of which about 20 are observed. Excitation with a green laser ($\lambda = 532$ nm) yields better resolved high-frequency modes, whereas red-laser excitation ($\lambda = 785$ nm) results in better resolved low-frequency modes. The assignment of bands was assisted by first-principles zone center phonon calculations. The modes with lowest and highest wave number were calculated at 168 and 683 cm^{-1}, respectively, which is in good agreement with the span of wave numbers of the observed spectrum. The bands in the wave number region 600–700 cm^{-1} correspond to B-Si vibrations (modes 14–19; Figure 2) and are detached from the bulk of modes between 150 and 470 cm^{-1}. The latter range of wave numbers is typical for Si-Si stretching and bending vibrations in silicide clathrates,[18] however, for $LiBSi_2$ we find that bands from Si-Si and Li-Si vibrations appear at similar wave numbers. In fact, mode 13 at around 467 cm^{-1} corresponds to a Li-Si vibration, whereas the first Si-Si stretching mode (12) is at around 430 cm^{-1}. This indicates a strong interaction between Li and the host OTF. Also, the optical mode with the lowest wave number involves displacement contributions from all atoms and is not, as perhaps expected, dominated by Li atoms.

The electronic structure of $LiBSi_2$ has been calculated and the density of states (DOS) is shown in Figure 3. $LiBSi_2$ is a semiconductor with a band gap of 1.1 eV. Because DFT-calculated band gaps are known to be underestimated, the

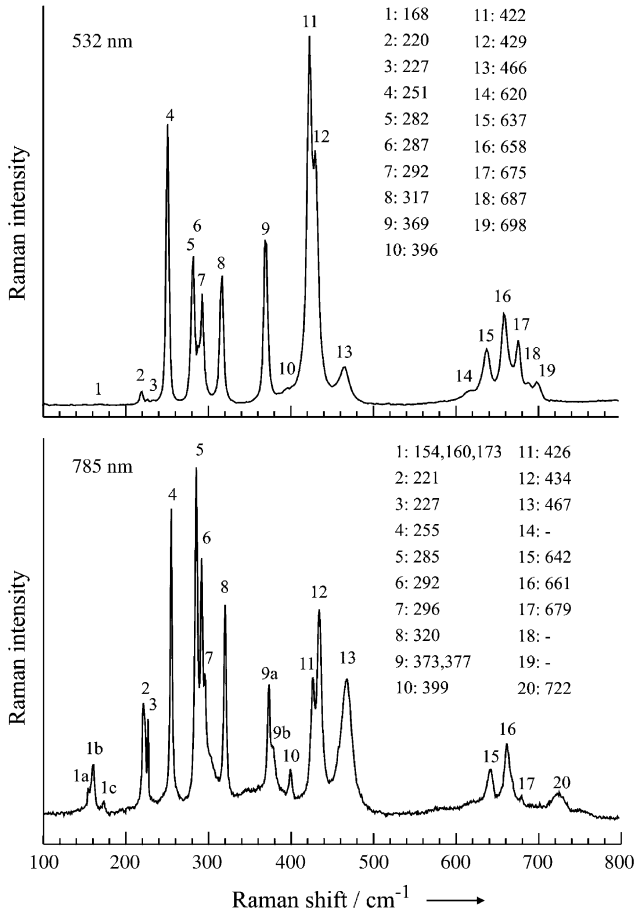

Figure 2. Raman spectrum of $LiBSi_2$ recorded with excitation wavelengths 532 and 785 nm. Values listed are wavenumbers (cm^{-1}) of the labeled bands (1–20). The origin of band 20 in the lower spectrum is not known.

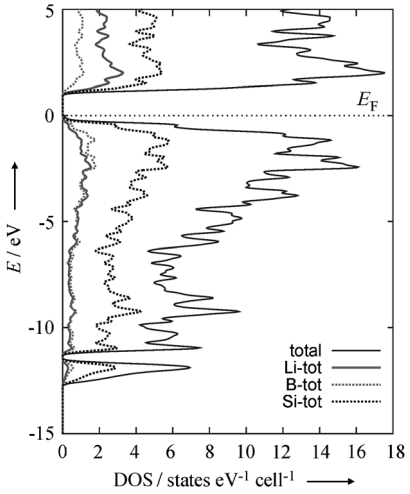

Figure 3. Electronic density of states for $LiBSi_2$ and the site projected contributions from Li, B, and Si atoms. The Fermi level (E_F) is set at 0 eV at the top of the valence band (dotted line).

experimental band gap may approach 2 eV. The occurrence of a band gap is in agreement with an electron precise B-Si OTF where Li acts as an electron donor, as expected for a Zintl phase. However, the site-projected DOS reveals that the Li and B states contribute almost equally and homogenously to the valence band throughout its range of dispersion. Such an intimate admixture of states from the less electronegative—electron-donating—component to the occupied valence band is not typical of a Zintl phase and is also indicative of strong Li-OTF interactions. Preliminary ^{7}Li- and ^{11}B-MAS-NMR investigations (chemical shift of ^{7}Li: −0.35 ppm) reveal the diamagnetic character. Further details on the NMR-spectroscopic investigations are given in the Supporting Information.

Apart from its new topology, the B-Si net in $LiBSi_2$ is also chemically unique: it represents the first example where B and Si atoms form an ordered common framework structure with boron exclusively engaged in heteronuclear B-Si contacts. Typically frameworks of borosilicides are characterized by either segregated B and Si structural entities or separated B_{12} icosahedra and Si_4 rhomboid rings as in β-SiB_3[19] or the occurrence of B/Si disorder as manifested in mixed occupied positions as, for example, in α-SiB_3, $Na_8B_{74.5}Si_{17.5}$,[20] and the earlier mentioned $K_7B_7Si_{39}$.[10] Since the **tum** net exclusively consists of four-connected nodes it additionally enlarges the number of models for novel tetrel allotropes, such as the recently predicted Si allotrope[21] or the experimentally established *m-allo*-Ge.[22]

In conclusion, we have shown that high-pressure reactions between LiB and Si afford $LiBSi_2$ with a novel intermetallic B-Si OTF dubbed **tum**. Unique to this compound is the encapsulation of small-sized Li as the guest species and the topology of the OTF, based on a strictly ordered distribution of B and Si atoms. Owing to the low density and its open framework structure, doped $LiBSi_2$ may be the basis for useful electrode materials.[9c] Also, **tum** may be an interesting model for a low-density allotrope of Group 14 elements. The search for such allotropes has recently become a very active field of research.[7,21] $LiBSi_2$ is predicted to be a semiconductor with a band gap exceeding 1 eV. Vibrational properties and the calculated electronic structure indicate that the Li guest species interacts strongly with the OTF host. The physical properties, the detailed formation conditions of $LiBSi_2$, as well as an analysis of the NMR-spectroscopic investigations will be presented in a forthcoming paper.

Experimental Section

In a typical synthesis a mixture of LiB and Si (80–100 mg, molar ratio 1:1) were sealed in a salt capsule. The capsules were compressed in a multi-anvil device[23] to a pressure of 10 GPa and subsequently heated to 900 °C at a rate of 5 °C min^{-1}. After equilibrating samples at their target temperature for one hour, the temperature was quenched and the pressure released at a rate of approximately 0.5 GPa per hour. The preparation of salt capsules and their recovery after high-pressure, high-temperature treatment was performed in an Ar-filled glove box. Thereafter, the product was treated with half concentrated HCl and washed several times with water and ethanol followed by drying in air. A synthesis run typically yielded 40–50 mg product. Products were analyzed by powder X-ray diffraction (PXRD), Raman, and ^{7}Li- and ^{11}B-MAS NMR spectroscopy.

Samples were ground, loaded into 0.3 mm capillaries, and measured on a STOE STADI P diffractometer (Ge-(111) monochromator for CuK_α radition, $\lambda = 1.54056$ Å) equipped with a linear position-sensitive detector (PSD). Tetragonal unit cell: $a =$ 6.83225(3) Å, $c = 8.83924(6)$ Å and space group $P4_2/nmc$. Further

details on the crystal structure may be obtained from the Fachinformationszentrum Karlsruhe, 76344 Eggenstein-Leopoldshafen, Germany (fax: (+49) 7247-808-666; e-mail: crysdata@fiz-karlsruhe.de), by quoting the depository number CSD-425643 ($LiBSi_2$).

Raman spectra were recorded on powder samples placed on a glass slide using a LabRAM HR 800 spectrometer with a back-thinned CCD detector and lasers at 532 and 785 nm as excitation sources. ^{7}Li- and ^{11}B-MAS (magic angle spinning) NMR spectra (Supporting Information, Figures S3,S4) were collected on a Varian VNMRs 500 spectrometer, operating at 160.37 MHz and 194.24 MHz for ^{11}B and ^{7}Li, respectively. MAS was performed at spinning speeds of 15–40 kHz with a Varian 1.6 mm triple resonance T^3-MAS probe. Theoretical calculations were performed in the framework of the frozen core all-electron projected augmented wave (PAW) method, as implemented in the program VASP.[24]

Received: February 22, 2013
Published online: April 22, 2013

Keywords: open tetrahedral frameworks · silicon · zeolites · Zintl phases

[1] a) J. V. Smith, *Chem. Rev.* **1988**, *88*, 149; b) M. O'Keeffe, B. G. Hyde, *Crystal Structures 1: Patterns and Symmetry*, Monograph, Mineralogical Assoc. of America, Washington DC, **1996**; c) O. Delgado Friedrichs, A. W. M. Dress, D. H. Huson, J. Klinowski, A. L. Mackay, *Nature* **1999**, *400*, 644.

[2] a) "Zintl Clathrates": A. V. Shevelkov, K. Kovnir in *Zintl Phases: Principles and Recent Developments*, *Vol. 139* (Eds.: D. M. P. Mingos, T. F. Fässler), Springer, Heidelberg **2011**, p. 97; b) "Structural Relationships Between Intermetallic Clathrates, Porous Tectosilicates and Clathrate Hydrates": D. Santamaria-Perez, F. Libeau in *Inorganic 3D Structures: The Extended Zintl-Klemm Concept*, *Vol. 138* (Eds.: D. M. P. Mingos, A. Vegas), Springer, Heidelberg **2011**, p. 1.

[3] Symbols for nets follow either the zeolite code according to ref. [3a] or the RCSR identifiers according to ref. [3b]; a) C. Baerlocher, W. M. Meier, D. H. Olson, *Atlas of Zeolite Framework Types*, 6th rev. ed., Elsevier, Amsterdam, **2007**. Data available online at http://www.iza-structure.org/databases/; b) M. O'Keeffe, M. A. Peskov, S. J. Ramsden, O. M. Yaghi, *Acc. Chem. Res.* **2008**, *41*, 1782.

[4] a) M. Beekman, G. S. Nolas, *J. Mater. Chem.* **2008**, *18*, 842; b) G. S. Nolas, J. L. Cohn, G. A. Slack, S. B. Schujman, *Appl. Phys. Lett.* **1998**, *73*, 178; c) S. Yamanaka, *Dalton Trans.* **2010**, *39*, 1901.

[5] a) W. Blase, G. Cordier, R. Kniep, R. Schmidt, *Z. Naturforsch. B* **1989**, *44*, 505; b) J. T. Vaughey, J. D. Corbett, *J. Am. Chem. Soc.* **1996**, *118*, 12098; c) W. Blase, G. Cordier, *Z. Naturforsch. B* **1988**, *43*, 1017; d) S. Stegmeier, S.-J. Kim, A. Henze, T. F. Fässler, unplublished results.

[6] a) J. D. Bryan, G. D. Stucky, *Chem. Mater.* **2001**, *13*, 253; b) W. Carrillo-Cabrera, S. Paschen, Y. Grin, *J. Alloys Compd.* **2002**, *333*, 4; c) A. Wosylus, Y. Prots, U. Burkhardt, W. Schnelle, U. Schwarz, *Sci. Technol. Adv. Mater.* **2007**, *8*, 383; d) A. Wosylus, Y. Prots, U. Burkhardt, W. Schnelle, U. Schwarz, Y. Grin, *Z. Naturforsch. B* **2006**, *61*, 1485; e) S. Yamanaka, S. Maekawa, *Z. Naturforsch. B* **2006**, *61*, 1493.

[7] a) M. M. J. Treacy, I. Rivin, E. Balkovsky, K. H. Randall, M. D. Foster, *Microporous Mesoporous Mater.* **2004**, *74*, 121; b) A. J. Karttunen, T. F. Fässler, M. Linnolahti, T. A. Pakkanen, *Inorg. Chem.* **2011**, *50*, 1733.

[8] Li replaces small amounts of Ge in the clathrate-I host structure. See: Y. Liang, B. Bohme, A. Ormeci, H. Borrmann, O. Pecher, F. Haarmann, W. Schnelle, M. Baitinger, Y. Grin, *Chem. Eur. J.* **2012**, *18*, 9818.

[9] a) A. Ker, E. Todorov, R. Rousseau, K. Uehara, F. X. Lannuzel, J. S. Tse, *Chem. Eur. J.* **2002**, *8*, 2787; b) N. Rey, A. Munoz, P. Rodriguez-Hernandez, A. San Miguel, *J. Phys. Condens. Matter* **2008**, *20*, 215218; c) A recent report gives evidence that Li can be inserted electrochemically into Si clathrate-II and may have potential as a novel electrode material for lithium-ion batteries, see: T. Langer, S. Dupke, H. Trill, S. Passerini, H. Eckert, R. Pöttgen, M. Winter, *J. Electrochem. Soc.* **2012**, *159*, A1318.

[10] W. Jung, J. Lorincz, R. Ramlau, H. Borrmann, Y. Prots, F. Haarmann, W. Schnelle, U. Burkhardt, M. Baitinger, Y. Grin, *Angew. Chem.* **2007**, *119*, 6846; *Angew. Chem. Int. Ed.* **2007**, *46*, 6725.

[11] a) F.O.X., Free Objects for Crystallography V 1.9.7.0, http://objcryst.sourceforge.net, **2011**; b) R. Černý, V. Favre-Nicolin, *Powder Diffr.* **2005**, *20*, 359; c) V. Favre-Nicolin, R. Cerny, *J. Appl. Crystallogr.* **2002**, *35*, 734; d) TOPAS 4.0—Rietveld Software, Bruker AXS, Madison (Wisconsin, USA), **2009**.

[12] Strong rings are defined as rings that are not the sum of any number of smaller cycles, see: O. Delgado-Friedrichs, M. O'Keeffe, *J. Solid State Chem.* **2005**, *178*, 2480.

[13] Realgar and Li_4 tetrahedral units have $-4m2$ symmetry. Note that the 4_2 screw axis runs through the centers of gravity of the $(Si1)_2$ units.

[14] a) V. A. Blatov, D. M. Proserpio, *Acta Crystallogr. Sect. A* **2009**, *65*, 202; b) V. A. Blatov, *IUCr CompComm. Newsletter* **2006**, *7*, 4; c) TOPOS Topological Databases and Topolgical Types Observed, http://www.topos.ssu.samara.ru.

[15] S. Ponou, S. J. Kim, T. F. Fässler, *J. Am. Chem. Soc.* **2009**, *131*, 10246.

[16] a) V. A. Blatov, O. Delgado-Friedrichs, M. O'Keeffe, D. M. Proserpio, *Acta Crystallogr. Sect. A* **2007**, *63*, 418; b) O. Delgado-Friedrichs, M. O'Keeffe, O. M. Yaghi, *Phys. Chem. Chem. Phys.* **2007**, *9*, 1035; c) V. A. Blatov, M. O'Keeffe, D. M. Proserpio, *CrystEngComm* **2010**, *12*, 44.

[17] E. Kroumova, C. Capillas, S. Ivantchev, H. Wondratschek, *Phase Transitions* **2003**, *76*, 155.

[18] a) G. S. Nolas, C. A. Kendziora, J. Gryko, J. Dong, C. W. Myles, A. Poddar, O. F. Sankey, *J. Appl. Phys.* **2002**, *92*, 7225; b) D. Machon, P. Toulemonde, P. F. McMillan, M. Amboage, A. Munoz, P. Rodriguez-Hernandez, A. San Miguel, *Phys. Rev. B* **2009**, *79*, 184101.

[19] J. R. Salvador, D. Bilc, S. D. Mahanti, M. G. Kanatzidis, *Angew. Chem.* **2003**, *115*, 1973; *Angew. Chem. Int. Ed.* **2003**, *42*, 1929.

[20] a) B. Magnusson, C. Brosset, *Acta Chem. Scand.* **1962**, *16*, 449; b) H. F. Rizzo, L. R. Bidwell, *J. Am. Ceram. Soc.* **1960**, *43*, 550; c) H. Morito, B. Eck, R. Dronskowski, H. Yamane, *Dalton Trans.* **2010**, *39*, 10197.

[21] a) M. A. Zwijnenburg, K. E. Jelfs, S. T. Bromley, *Phys. Chem. Chem. Phys.* **2010**, *12*, 8505; b) C. J. Pickard, R. J. Needs, *Phys. Rev. B* **2010**, *81*, 014106.

[22] a) A. Grüttner, R. Nesper, H. G. von Schnering, *Angew. Chem.* **1982**, *94*, 933; *Angew. Chem. Int. Ed. Engl.* **1982**, *21*, 912; b) F. Kiefer, A. J. Karttunen, M. Döblinger, T. F. Fässler, *Chem. Mater.* **2011**, *23*, 4578.

[23] E. Stoyanov, U. Häussermann, K. Leinenweber, *High Pressure Res.* **2010**, *30*, 175.

[24] a) P. E. Blöchl, *Phys. Rev. B* **1994**, *50*, 17953; b) G. Kresse, D. Joubert, *Phys. Rev. B* **1999**, *59*, 1758; c) G. Kresse, J. Hafner, *Phys. Rev. B* **1993**, *48*, 13115; d) G. Kresse, J. Furthmüller, *Comput. Mater. Sci.* **1996**, *6*, 15.

